Supporting Information

Facile immobilization of P^NN^NP-Pd pincer complexes in MFU-4*l*-OH and the effects of guest loading on Lewis acid catalytic activity

Jordon S. Hilliard and Casey R. Wade*

Department of Chemistry and Biochemistry, The Ohio State University, Columbus, Ohio 43210, United States

*E-mail: wade.521@osu.edu

Table of Contents:

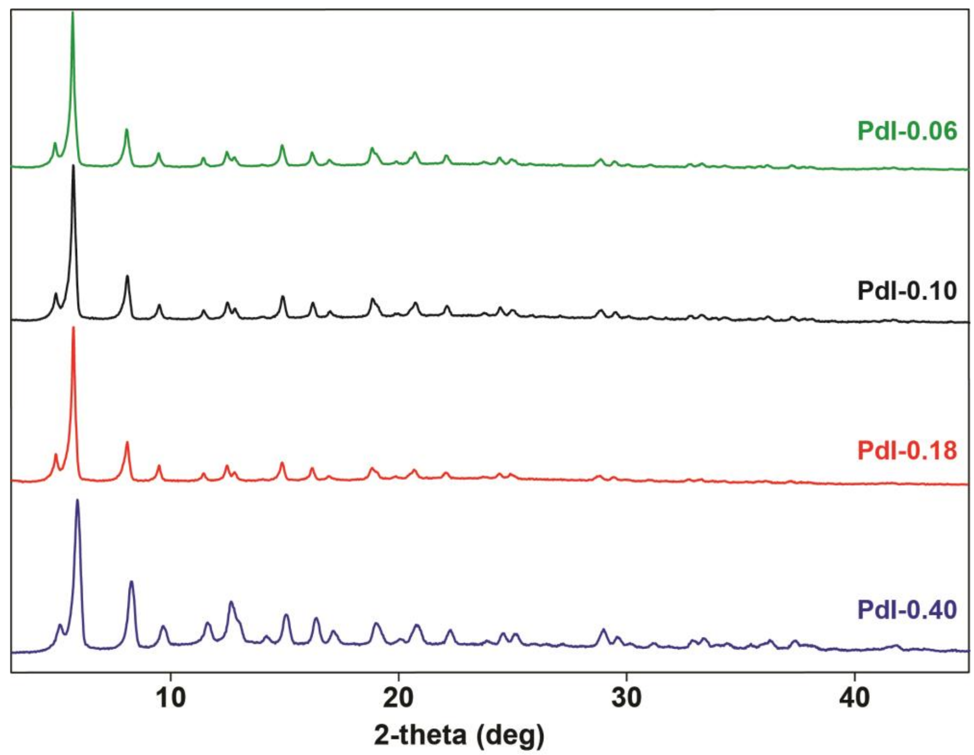

Figure S1. PXRD patterns of PdI-x

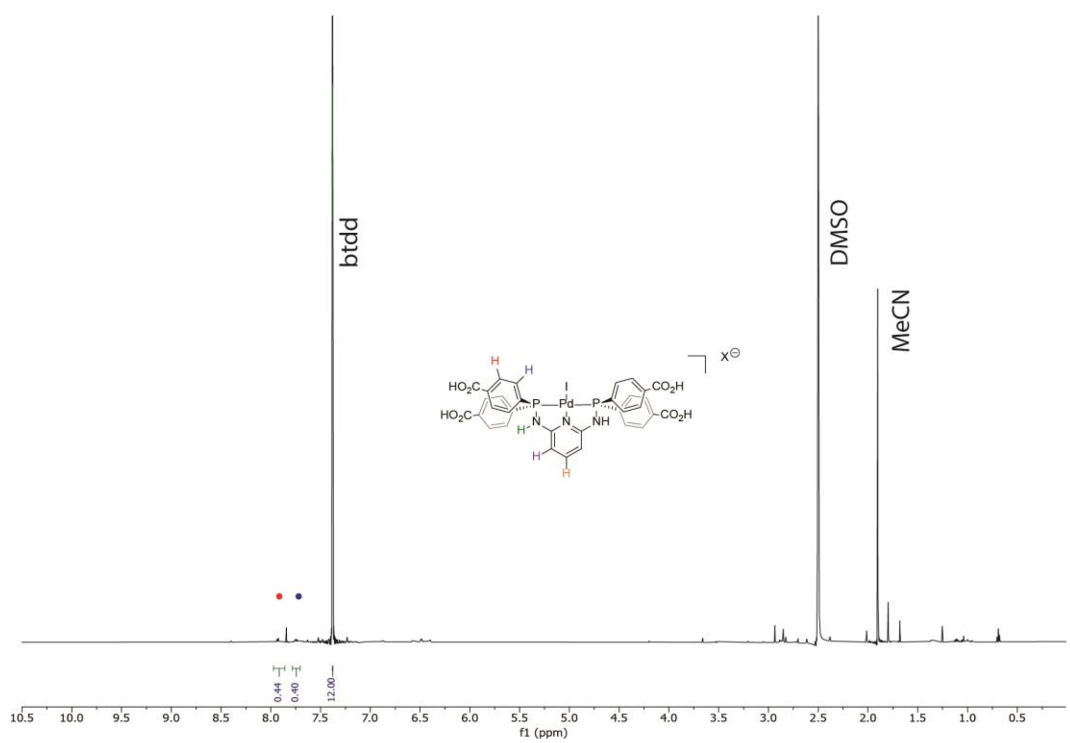

Figure S2. Acid-digested [1]H NMR spectrum (CF_3CO_2H/ DMSO-d_6) of **PdI-0.06**

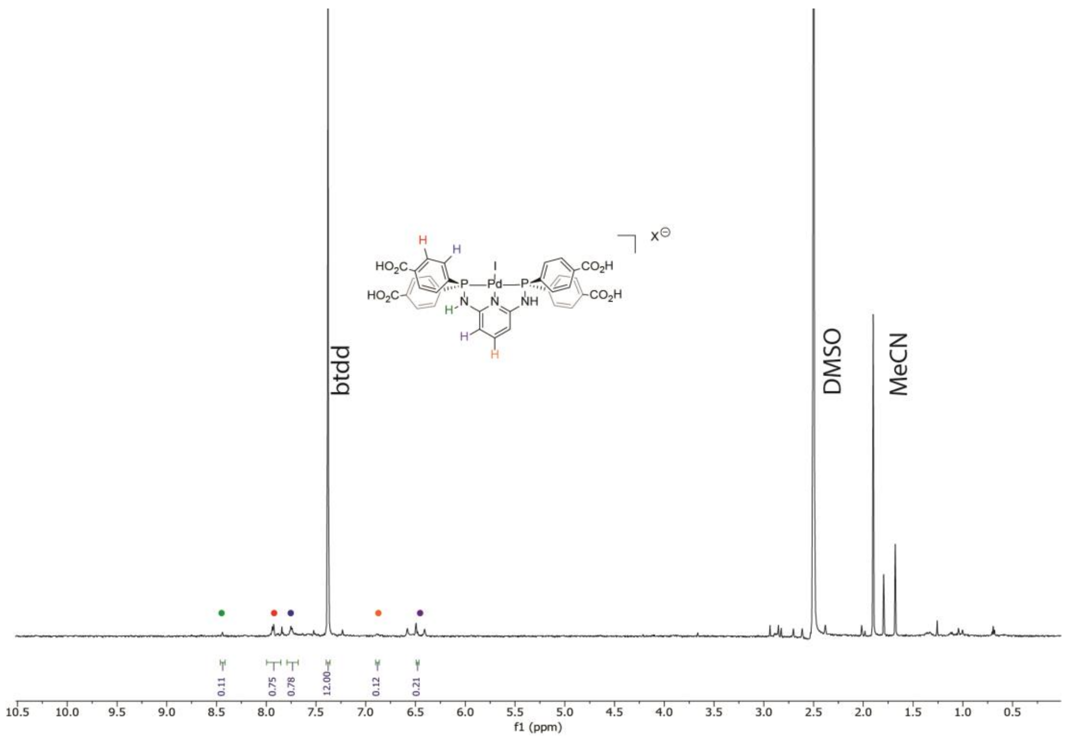

Figure S3. Acid-digested ^{1}H NMR spectrum (CF_3CO_2H/ DMSO-d_6) of **PdI-0.10**

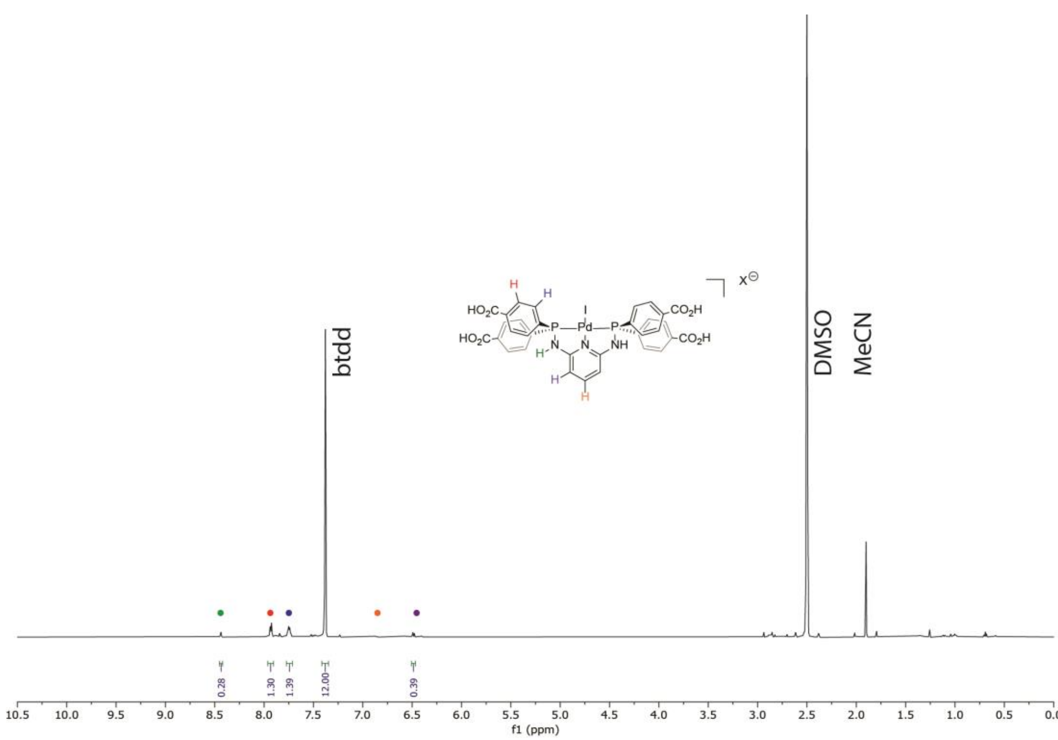

Figure S4. Acid-digested ^{1}H NMR spectrum (CF_3CO_2H/ DMSO-d_6) of **PdI-0.18**

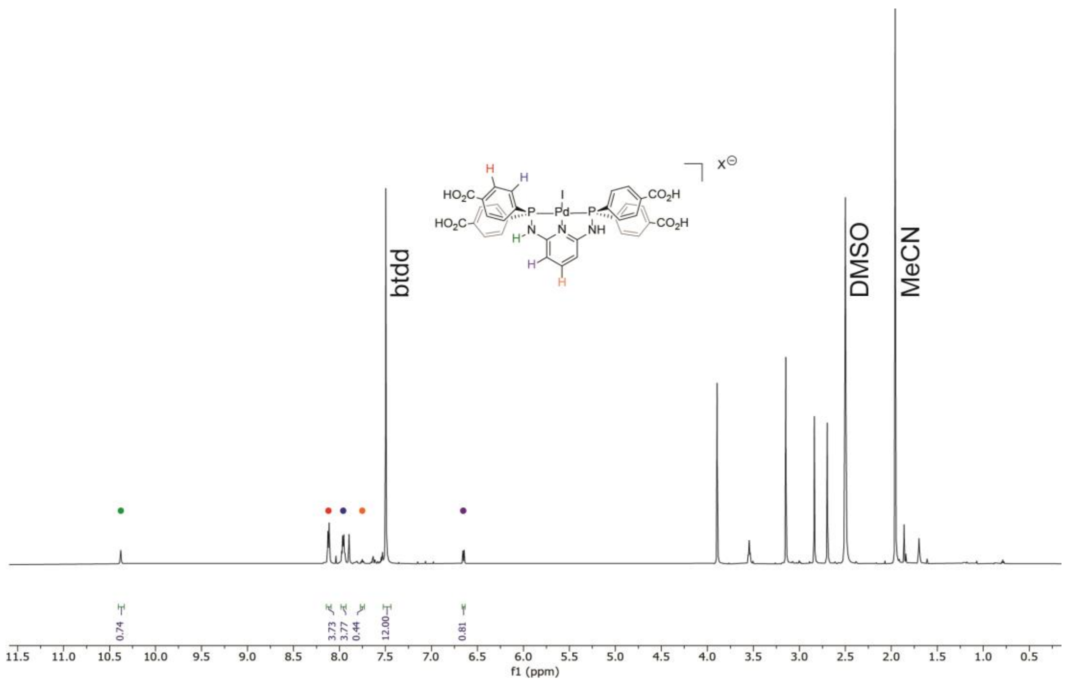

Figure S5. Acid-digested ^{1}H NMR spectrum (CF_3CO_2H/ DMSO-d_6) of **PdI-0.40**

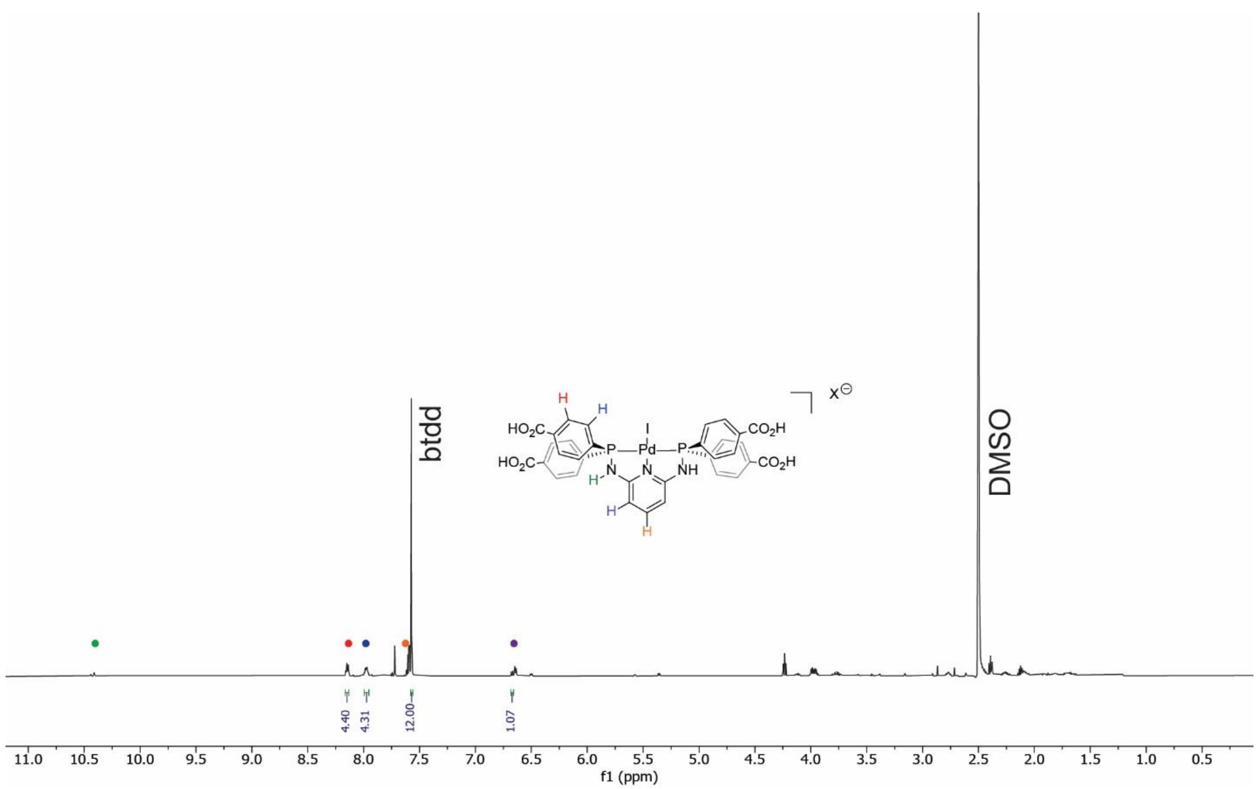

Figure S6. Acid-digested ^{1}H NMR spectrum (CF_3CO_2H/ DMSO-d_6) of **PdI-0.50**

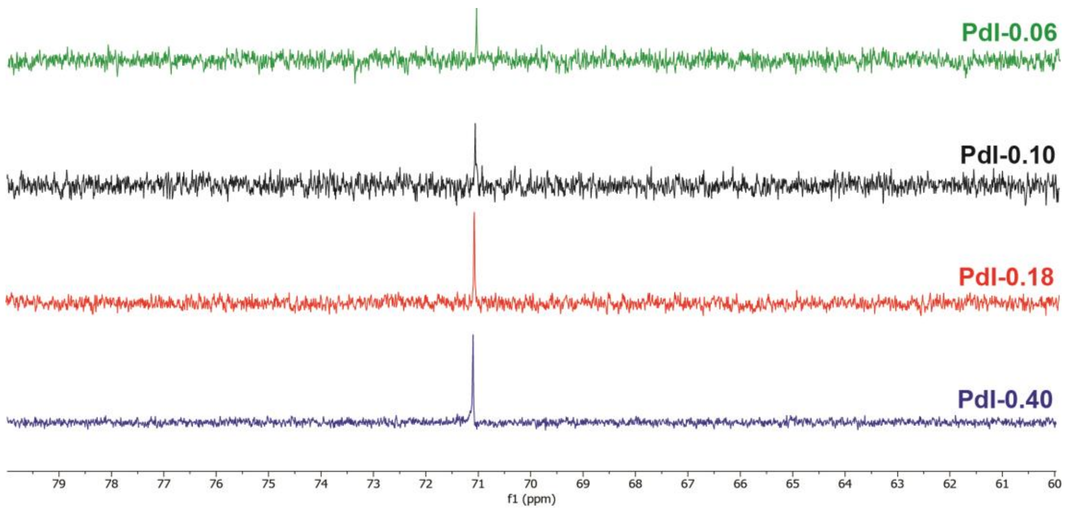

Figure S7. Acid-digested $^{31}P\{^{1}H\}$ NMR spectra (CF_3CO_2H/DMSO-d_6) of **PdI-x**

Entry	Equiv. of $H_3(P^NN^NP\text{-PdI})$ added to MFU-4*l*-OH	Equiv. of $H_3(P^NN^NP\text{-PdI})$ adsorbed
1	0.06	0.06
2	0.10	0.10
3	0.16	0.16
4	0.18	0.18
5	0.25	0.25
6	0.40	0.40
7	1.00	0.50
8	1.00 (MFU-4*l*-Cl)	0.00

Figure S8. Quantification of $H_3(P^NN^NP\text{-PdI})$ adsorbed in MFU-4*l*-OH upon reaction with varying amounts of complex. The amount of $H_3(P^NN^NP\text{-PdI})$ added/adsorbed is given as equivalents per formula unit MOF ($Zn_5(OH)_4(btdd)_3$).

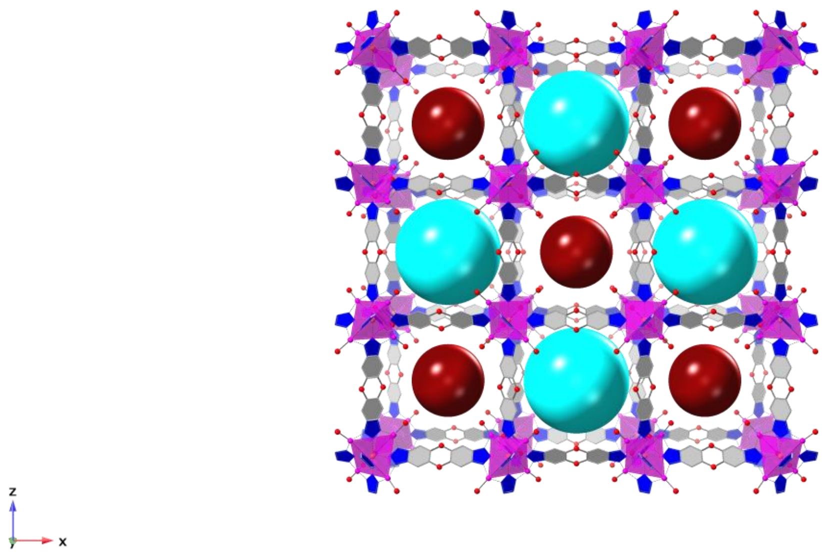

Figure S9. Alternating pore structure of MFU-4*l*-OH showing the Type A (~12 Å, red) and Type B (~18 Å, cyan) pores.

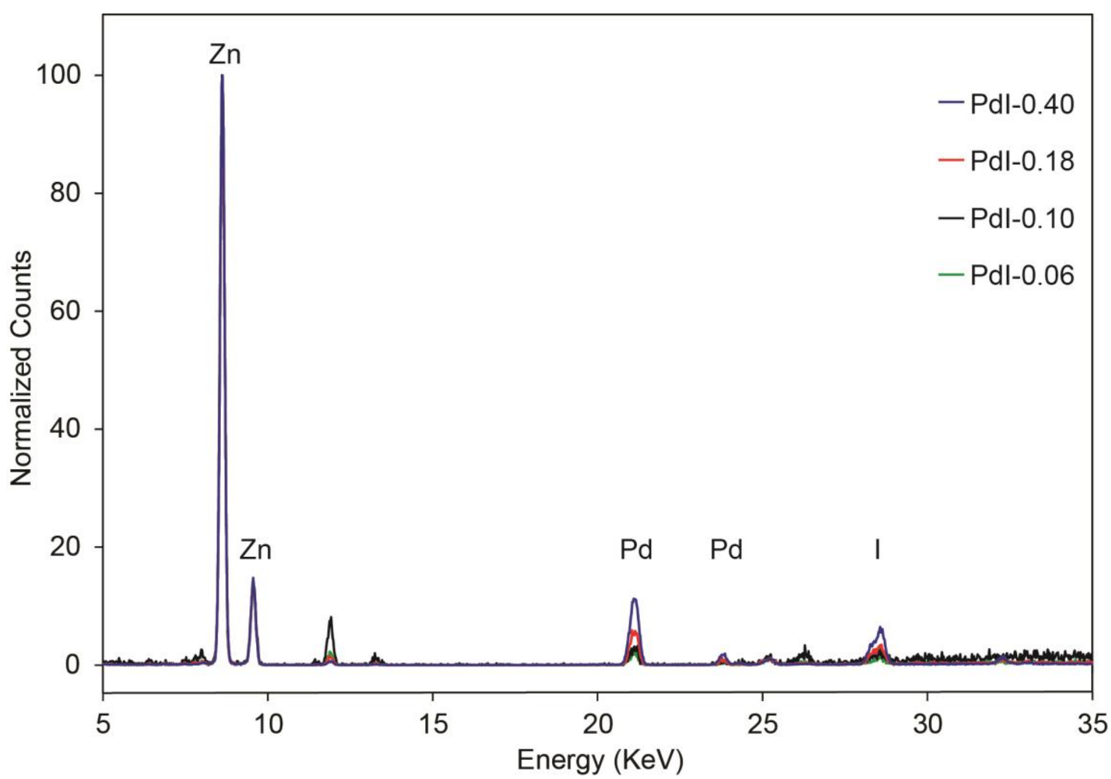

Figure S10. XRF spectra of **PdI-x**

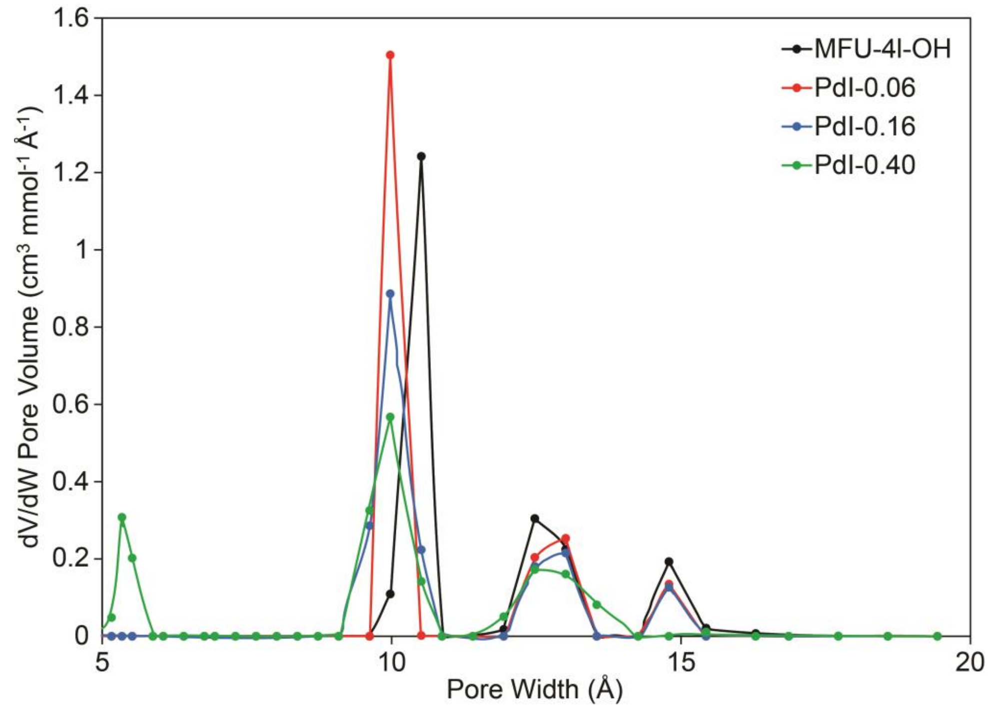

Figure S11. DFT differential pore volume plots for MFU-4*l*-OH, **PdI-0.06**, **PdI-0.16**, and **PdI-0.40** calculated using the infinite slit adsorption model with 2D-non-local density functional theory.

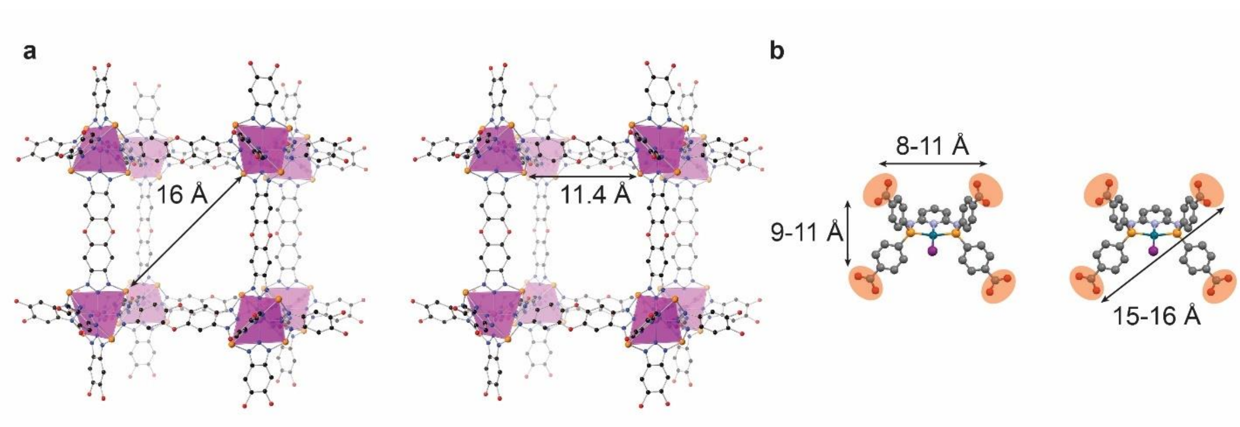

Figure 12. a) Approximate Zn···Zn intercluster distances in the Zn–OH functionalized pore of MFU-4*l*-OH. b) Approximate distances between the carboxylic acid groups of H_3(PNNNP-PdI).

The similarity between the MFU-4*l*-OH intercluster distances and distances between the carboxylic acid groups of H_3(PNNNP-PdI) support the notion that the encapsulated PNNNP-PdI complex can simultaneously bind to multiple Zn sites of the node.

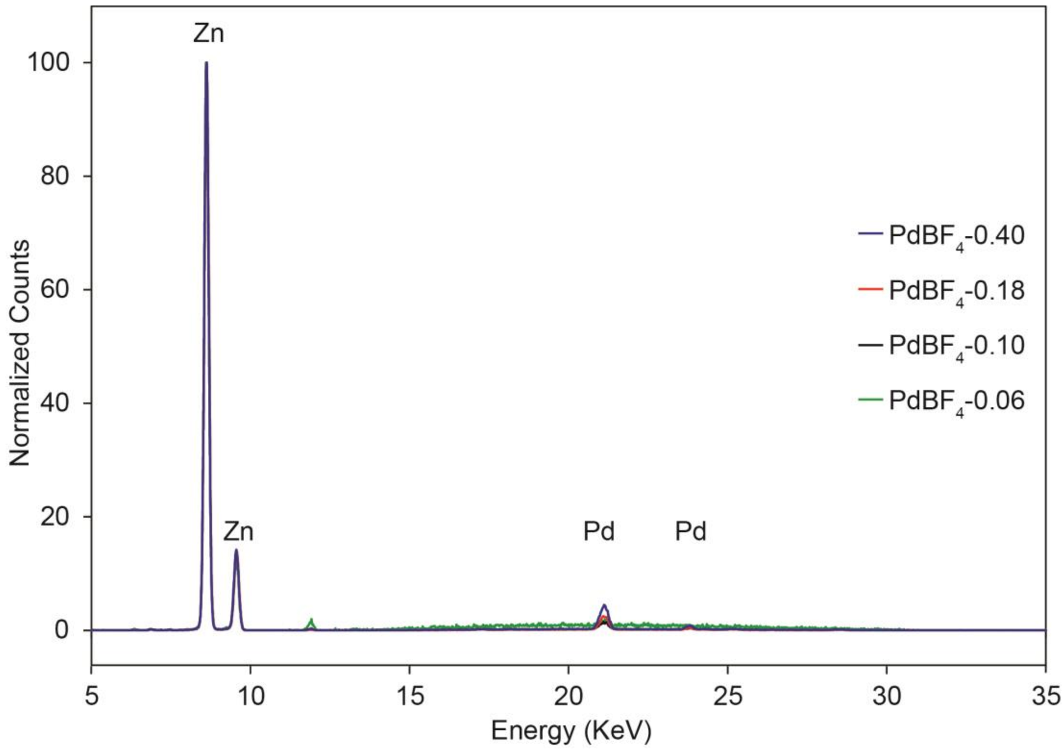

Figure S13. XRF spectra of **$PdBF_4$-x**

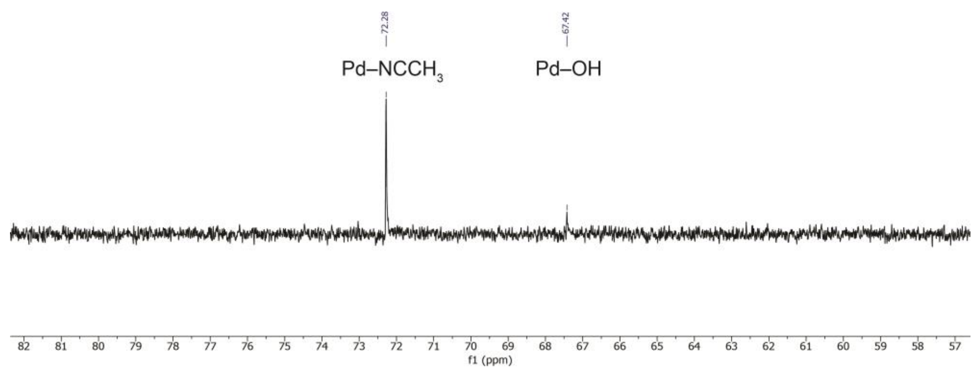

Figure S14. Acid-digested $^{31}P\{^{1}H\}$ NMR spectrum (CF_3CO_2H/DMSO-d_6) of **$PdBF_4$-0.40**

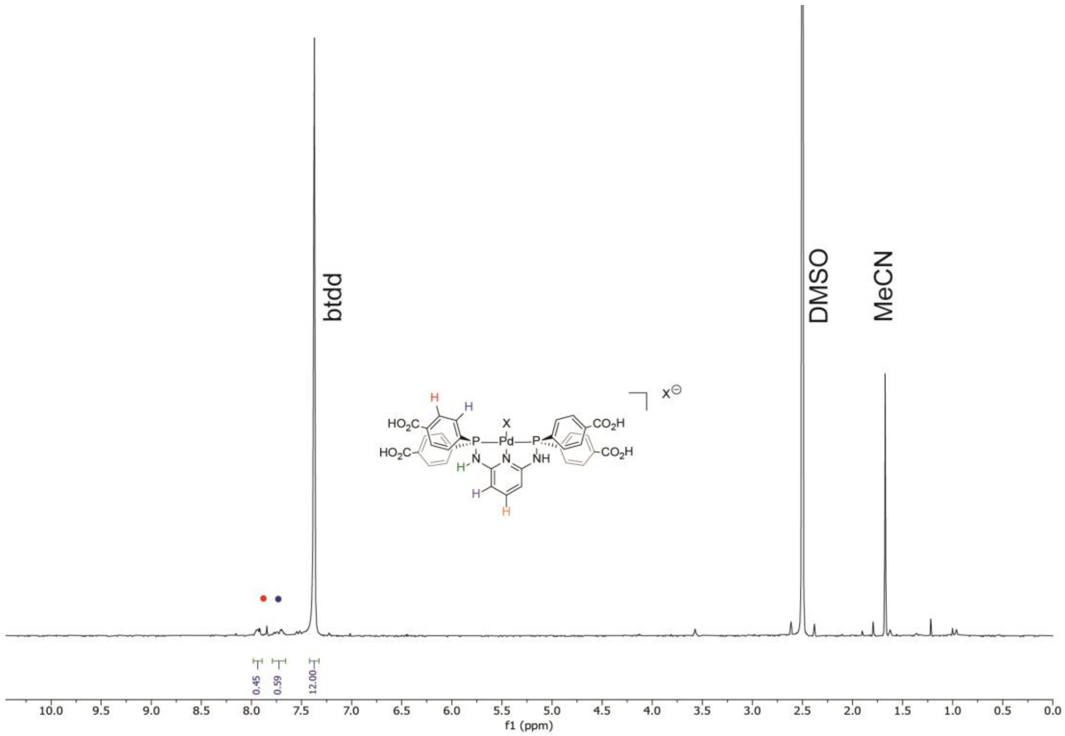

Figure S15. Acid digested [1]H NMR spectrum (CF_3CO_2H/ DMSO-d_6) of **$PdBF_4$-0.06**

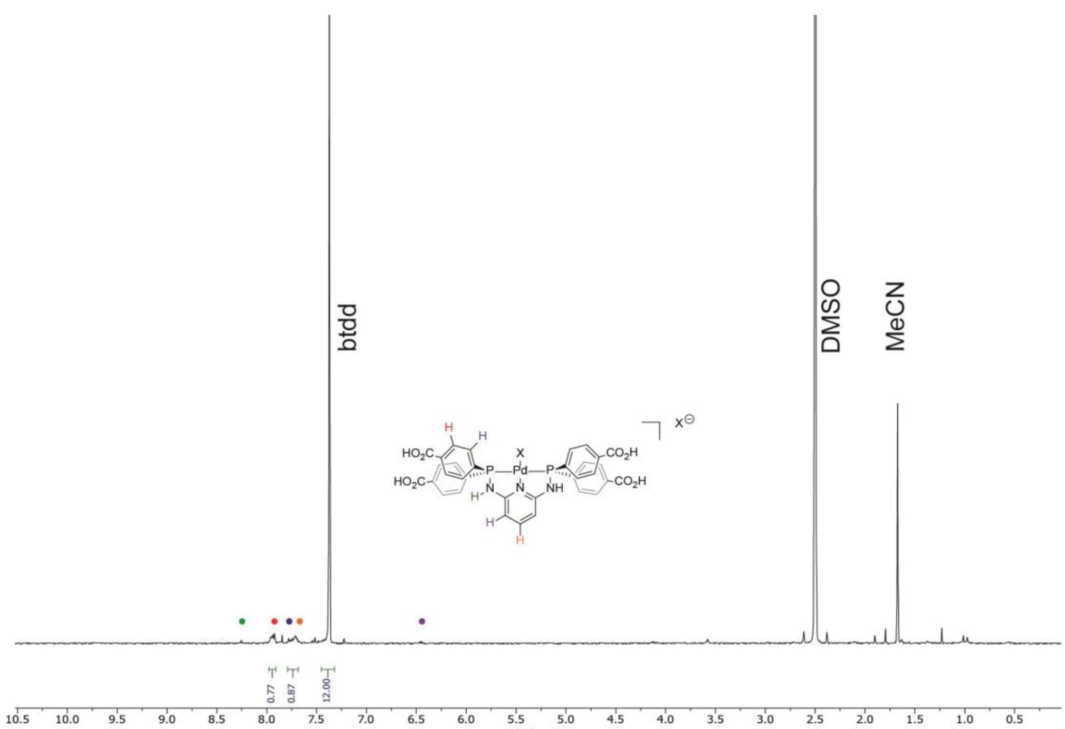

Figure S16. Acid digested [1]H NMR spectrum (CF_3CO_2H/ DMSO-d_6) of **$PdBF_4$-0.10**

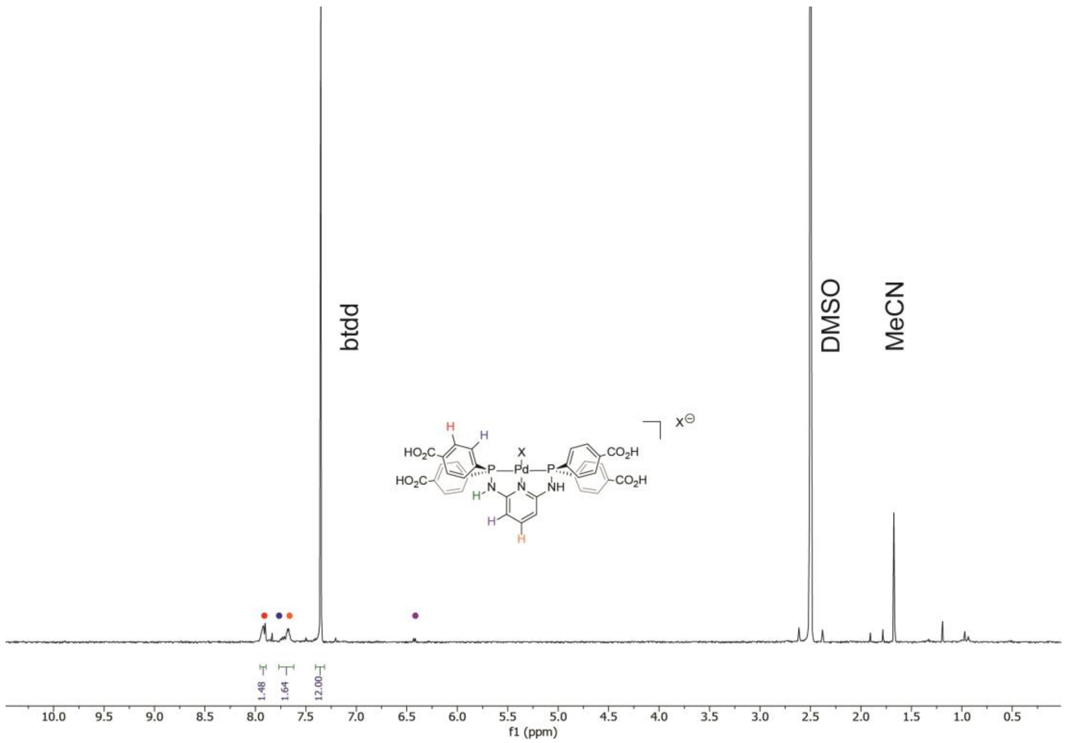

Figure S17. Acid digested [1]H NMR spectrum (CF_3CO_2H/ DMSO-d_6) of **$PdBF_4$-0.18**

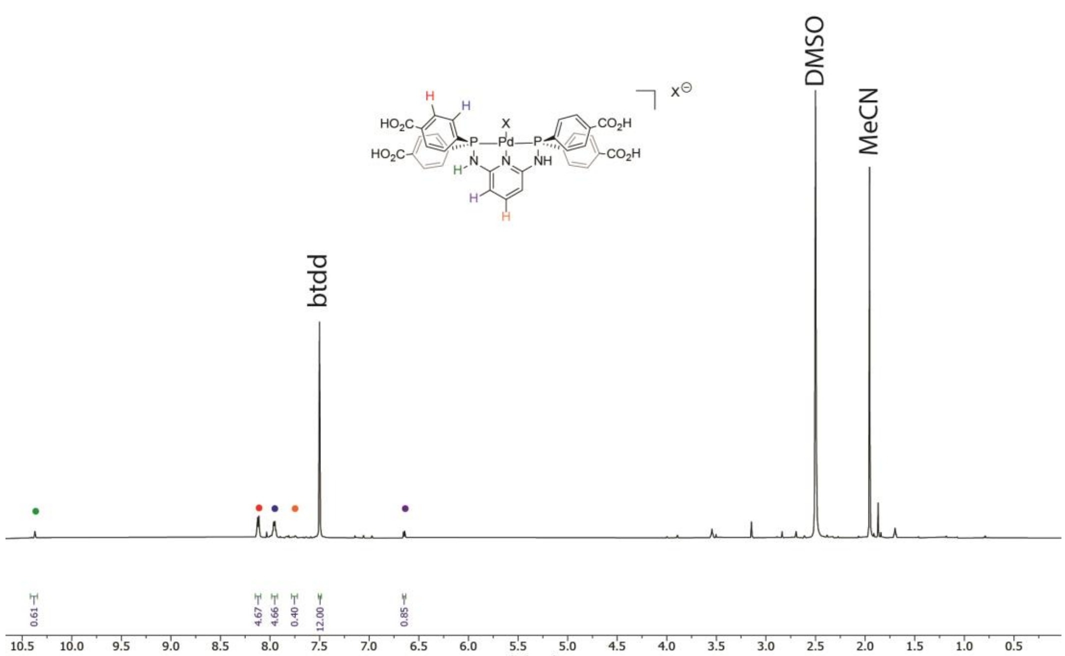

Figure S18. Acid digested [1]H NMR spectrum (CF_3CO_2H/DMSO) of **$PdBF_4$-0.40**

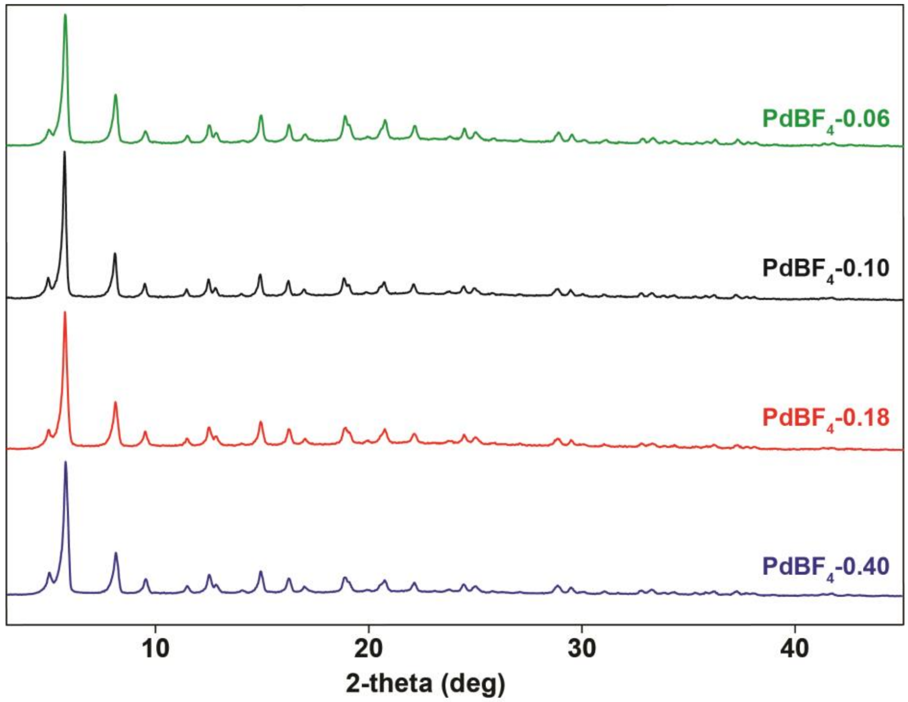

Figure S19. PXRD patterns of **$PdBF_4$-x**

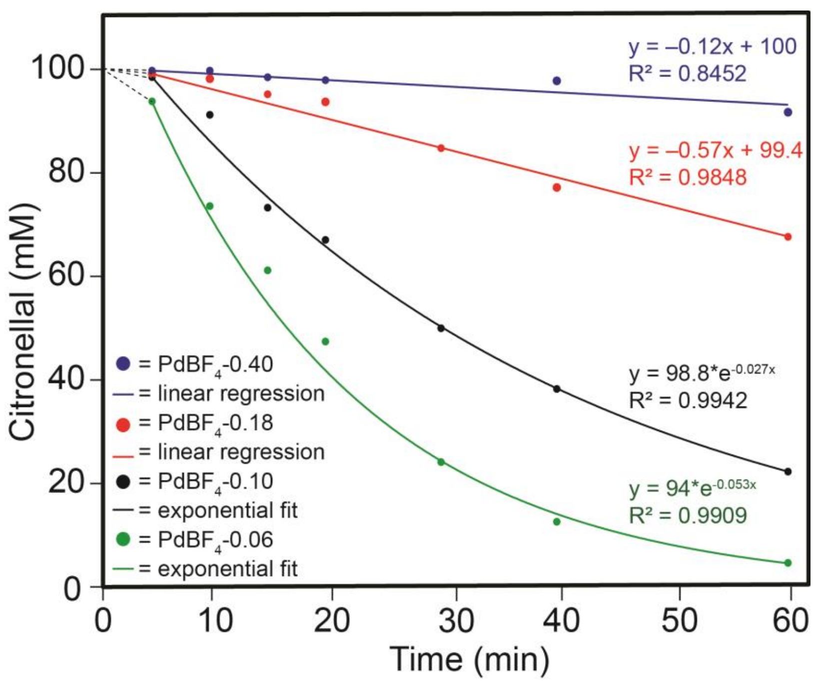

Figure S20. Experimental kinetic data collected during the catalytic cyclization of citronellal (100 mM) with **$PdBF_4$-x** (0.5 mol % Pd) using a single term exponential fit at loadings of x = 0.06 (green) and 0.10 (black) equiv. Pd per formula unit. At loadings of x = 0.18 (red) and 0.40 (blue) equiv. Pd per formula unit, a linear regression model is used for fitting.

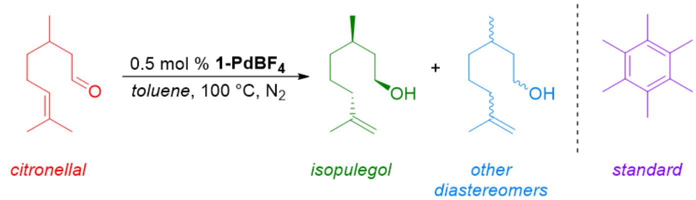

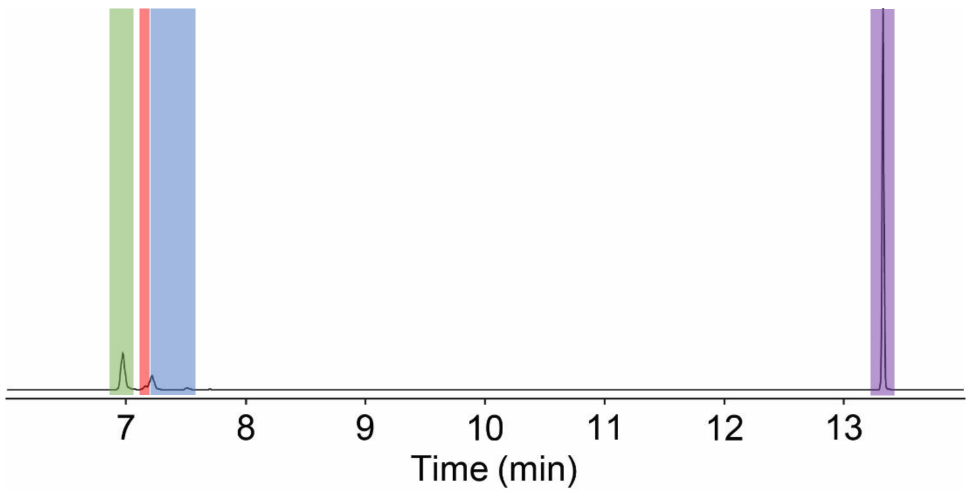

Substrate	Retention Time (min)	Integration (a.u)	Response Factor	Yield (%)
Isopulegol	6.987	390229	1.98	62
Citronellal	7.182	31803	1.98	5
Diastereomers	7.233-7.720	205349	1.98	33
Hexamethylbenzene	13.322	1845798	1.00	—

Figure S21. GC-FID trace of the carbonyl-ene cyclization of citronellal with **$PdBF_4$-0.06** (0.5 mol % Pd) (0.2 mmol hexamethylbenzene internal standard)

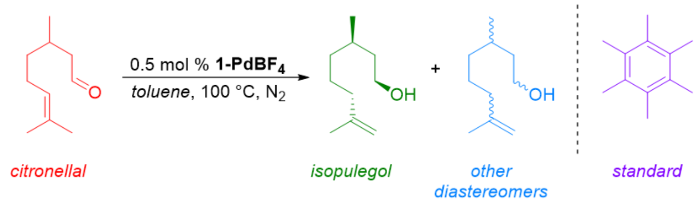

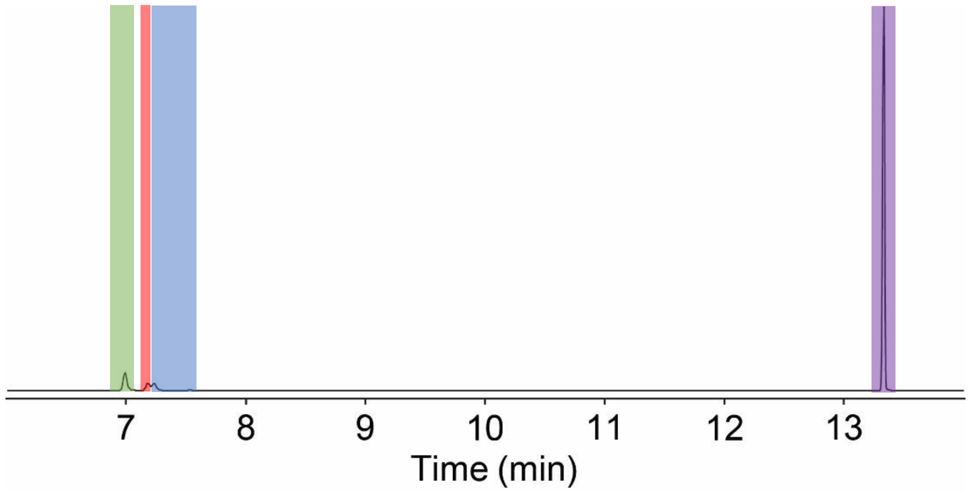

Substrate	Retention Time (min)	Integration (a.u)	Response Factor	Yield (%)
Isopulegol	6.987	268065	1.98	51
Citronellal	7.182	120160	1.98	22
Diastereomers	7.233-7.720	142103	1.98	27
Hexamethylbenzene	13.322	2803957	1.00	—

Figure S22. GC-FID trace of the carbonyl-ene cyclization of citronellal with **$PdBF_4$-0.10** (0.5 mol % Pd) (0.2 mmol hexamethylbenzene internal standard)

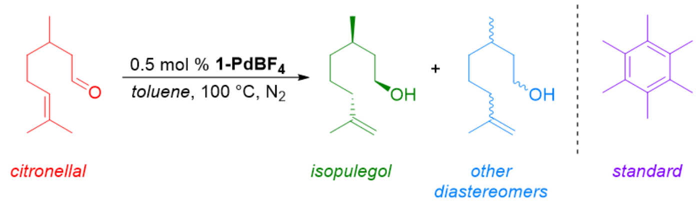

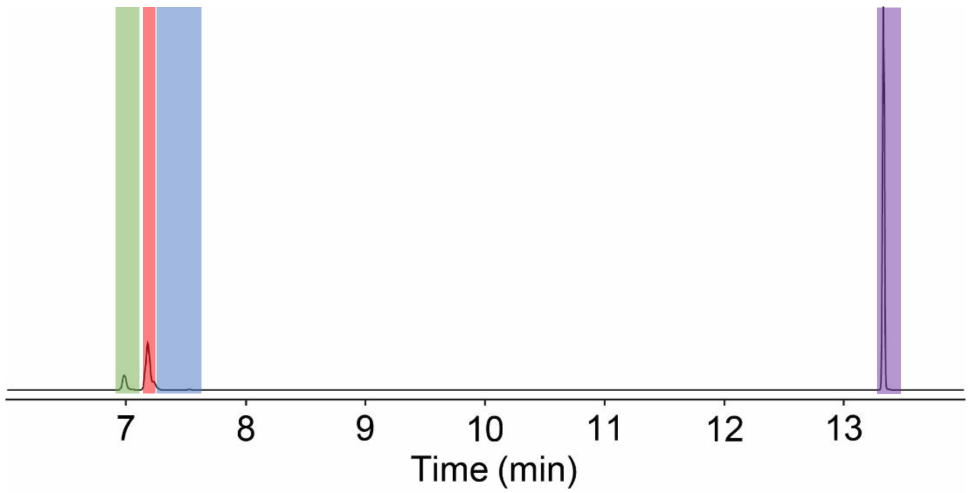

Substrate	Retention Time (min)	Integration (a.u)	Response Factor	Yield (%)
Isopulegol	6.987	206918	1.98	21
Citronellal	7.182	678981	1.98	68
Diastereomers	7.233-7.720	113207	1.98	11
Hexamethylbenzene	13.322	2455973	1.00	—

Figure S23. GC-FID trace of the carbonyl-ene cyclization of citronellal with **$PdBF_4$-0.18** (0.5 mol % Pd) (0.2 mmol hexamethylbenzene internal standard)

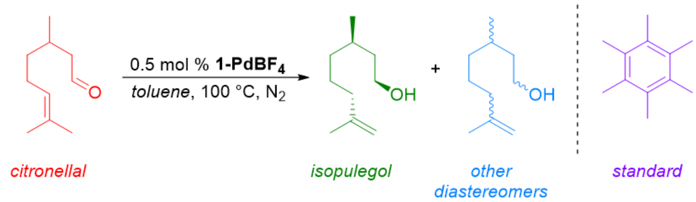

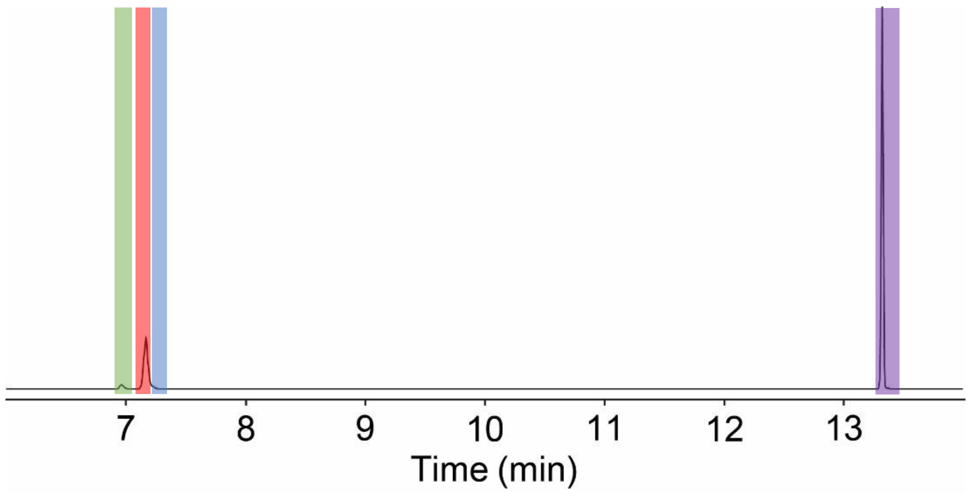

Substrate	Retention Time (min)	Integration (a.u)	Response Factor	Yield (%)
Isopulegol	6.987	77705	1.98	7.6
Citronellal	7.182	941518	1.98	92
Diastereomers	7.233-7.720	4288	1.98	0.4
Hexamethylbenzene	13.322	3282212	1.00	—

Figure S24. GC-FID trace of the carbonyl-ene cyclization of citronellal with **PdBF₄-0.40** (0.5 mol % Pd) (0.2 mmol hexamethylbenzene internal standard)

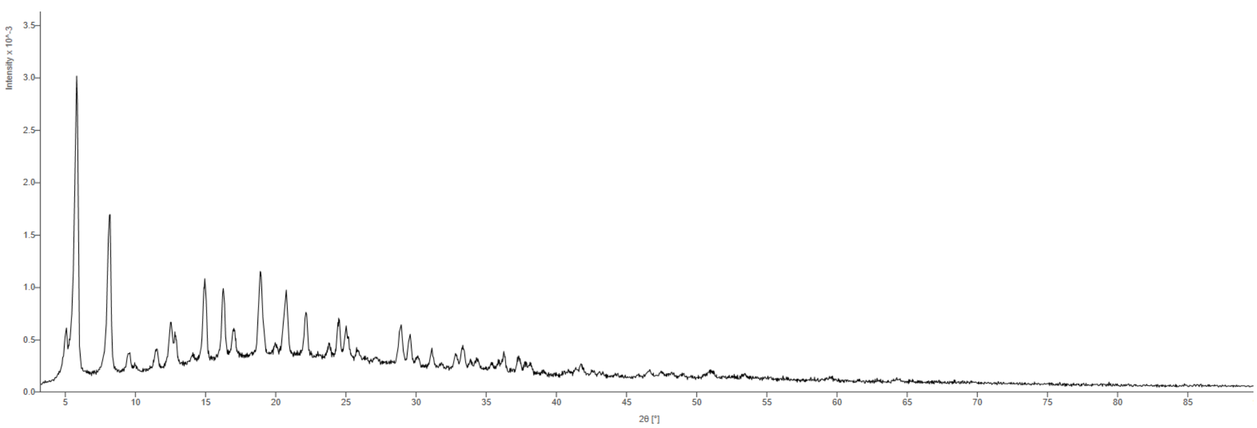

Figure S25. PXRD pattern of **PdBF₄-0.06** after recyclability studies

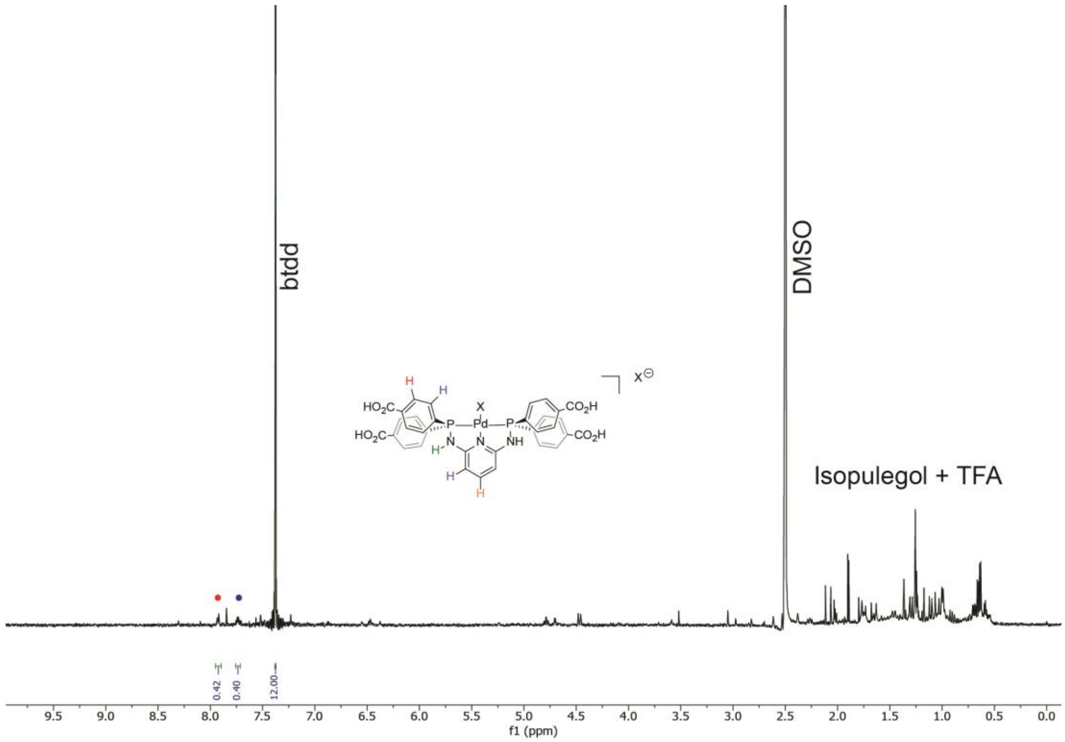

Figure S26. Acid digested [1]H NMR spectrum (CF_3CO_2H/ DMSO-d_6) of **$PdBF_4$-0.06** after catalysis

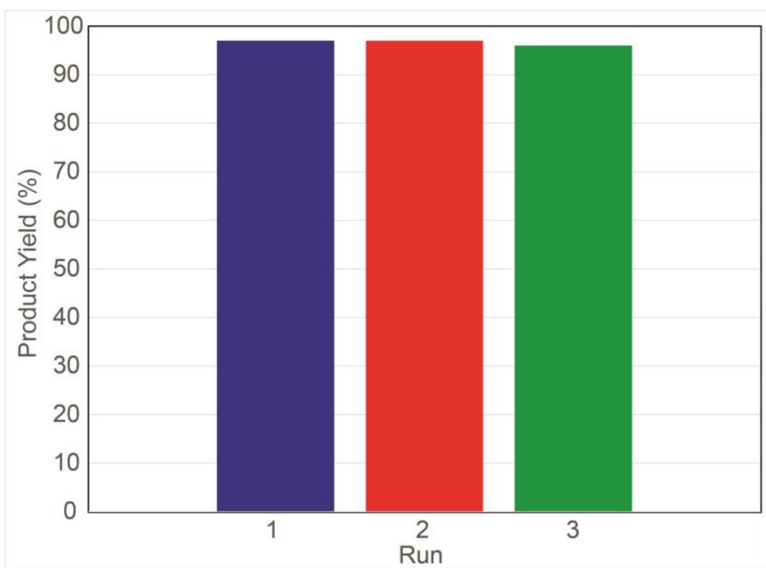

Figure S27. Experimental data collected for recycled catalyst during the cyclization of citronellal (100 mM) with **$PdBF_4$-0.06**

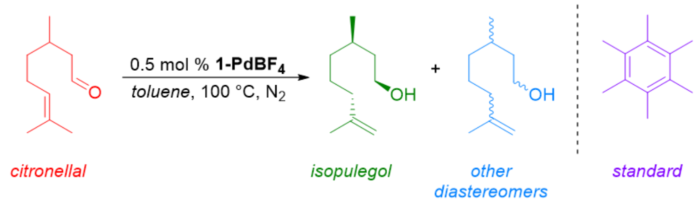

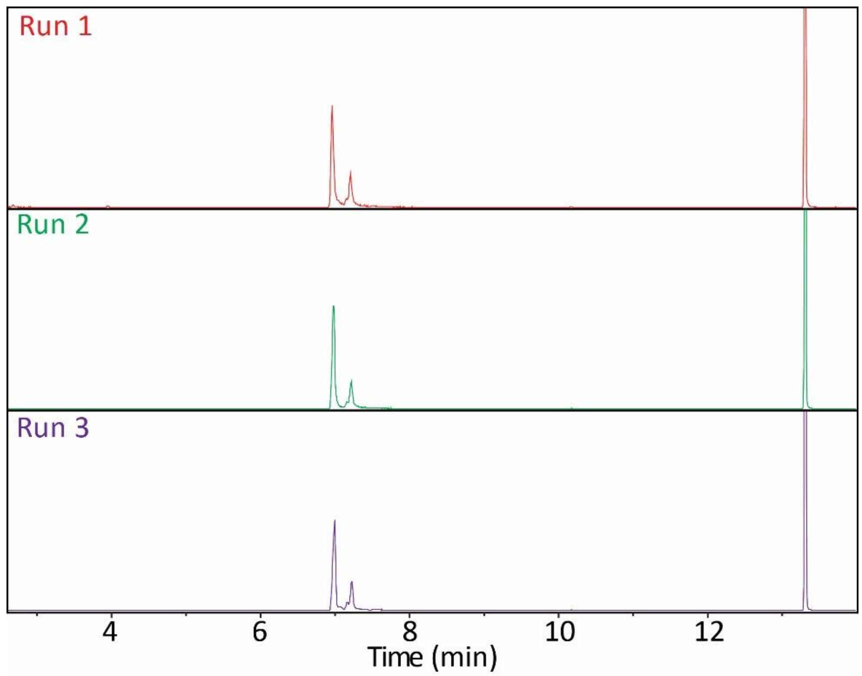

Analyte	Retention Time (min)	Response Factor	Integration Run 1	Yield (%) Run 1	Integration (a.u) Run 2	Yield (%) Run 2	Integration Run 3	Yield (%) Run 3
Isopulegol	6.987	1.98	179397	74.6	796064	77.9	1176068	74.9
Citronellal	7.182	1.98	7123	3.0	34737	3.4	68142	4.3
Diastereomers	7.233-7.720	1.98	54039	22.4	190969	18.7	326638	20.8
Hexamethylbenzene	13.322	1.00	1057531	—	3789368	—	5611119	—

Figure S28. GC-FID data collected for the catalyst recycling studies with **$PdBF_4$-0.06** (0.5 mol % Pd, 0.2 mmol hexamethylbenzene internal standard).

Procedure for hot filtration test. The catalytic citronellal cyclization reaction was prepared as described in the Experimental section with **PdBF$_4$-0.18** (0.5 mol % Pd) following minor modifications. A 100 mM solution of citronellal in toluene containing a known amount of hexamethylbenzene as an internal standard was combined with 0.5 mol% **PdBF$_4$-0.18**. The reaction mixture was heated and monitored by GC-FID to determine product yields. After 20 minutes, the reaction mixture was decanted from the solid MOF and filtered through a 0.45 μm syringe filter. The reaction was transferred to a clean vial, sealed, and allowed to proceed for an additional 40 minutes. Reaction aliquots were periodically characterized by GC-FID and showing no substrate conversion after removal of the MOF catalyst.

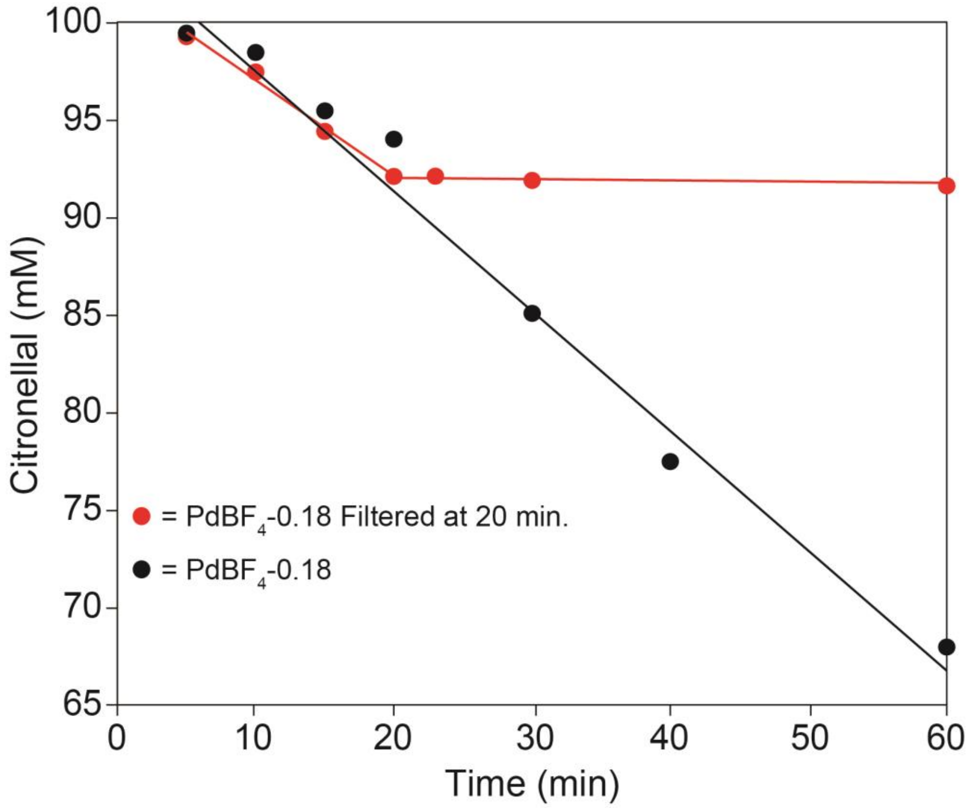

Figure S29. Experimental data collected during hot filtration test for the cyclization of citronellal (100 mM) with **PdBF$_4$-0.18**

Entry	Catalyst	mmol·g_{cat}^{-1}·h^{-1}	Ref
1	$PdBF_4$-0.06	9.16	--
2	$PdBF_4$-0.10	12.20	--
3	$PdBF_4$-0.18	8.48	--
4	$PdBF_4$-0.40	4.10	--
5	Sn-beta (Si:Sn 82)	341.17	1
7	MOF-808-2.5SO4	83.10	2
9	hcp UiO-66	9.60	3
10	UiO-66	8.83	3
11	UiO-66-NO_2	4.93	4
12	UiO-66-NO_2-10_{HCl}	2.14	5
13	Dehydrated UiO-66	1.32	6
14	UiO-66-350	1.00	7
15	Pd@MIL-101-Cr	0.92	8
16	MIL-101-Cr	0.62	8
17	Zr-Ti-NDC	0.56	9
18	$Cu_3(btc)_2$	0.55	10
19	Hydrated UiO-66	0.43	6
20	MIL-100(Fe)	0.18	11

Figure S30. Literature examples of heterogenous catalysts for the cyclization of citronellal. Activity is reported as mmol of substrate consumed per gram of catalyst per hour (mmol·g_{cat}^{-1}·h^{-1}).

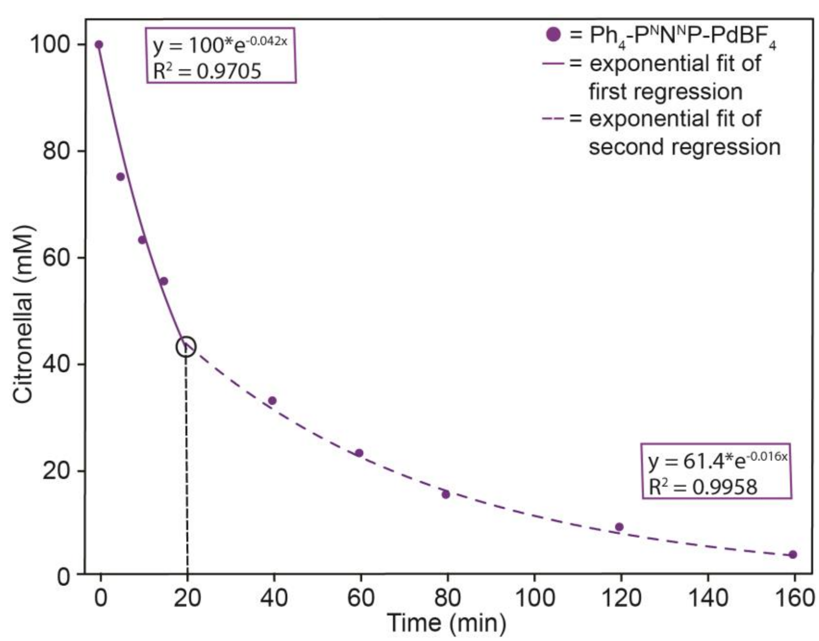

Figure S31. Experimental data collected during the cyclization of citronellal (100 mM) with **Ph_4-P^NN^NP-$PdBF_4$** (0.5 mol % Pd) using single term exponential fits.

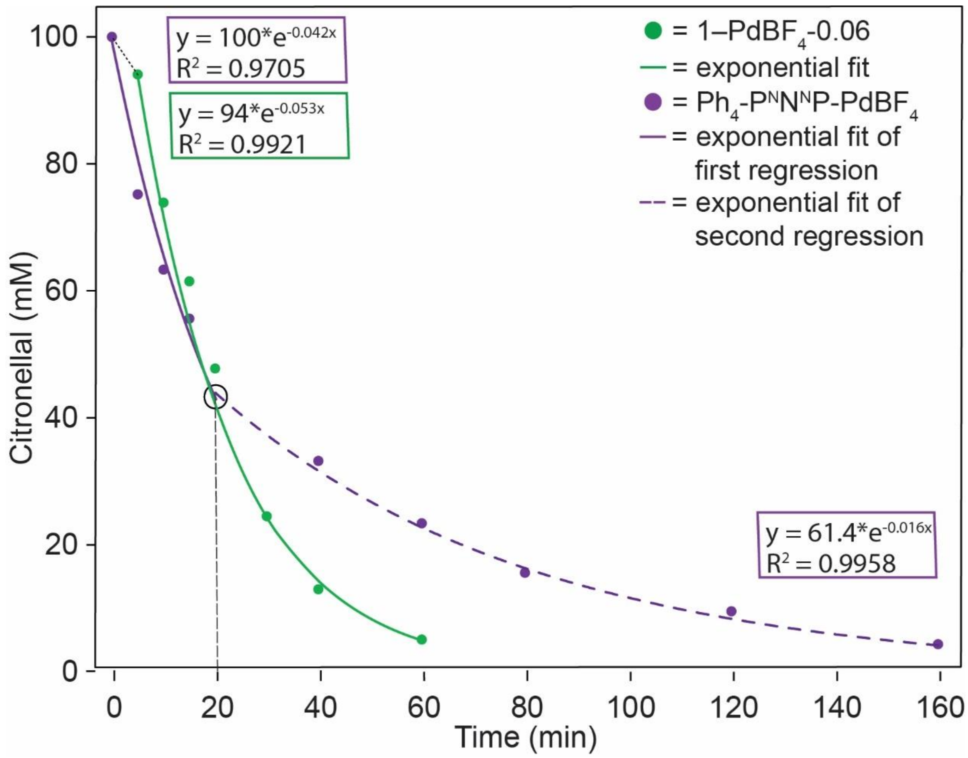

Figure S32. Experimental data collected during the catalytic cyclization of citronellal (100 mM) with **$PdBF_4$-0.06** (0.5 mol % Pd) using a single term exponential fit (green) and **Ph_4-P^NN^NP-$PdBF_4$** using two separate single term exponential fits (purple).

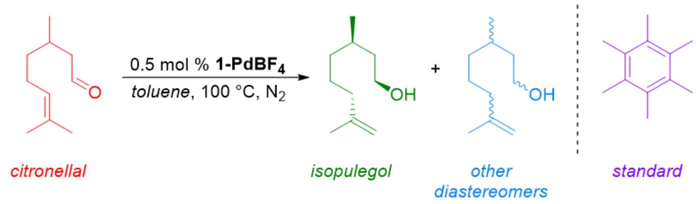

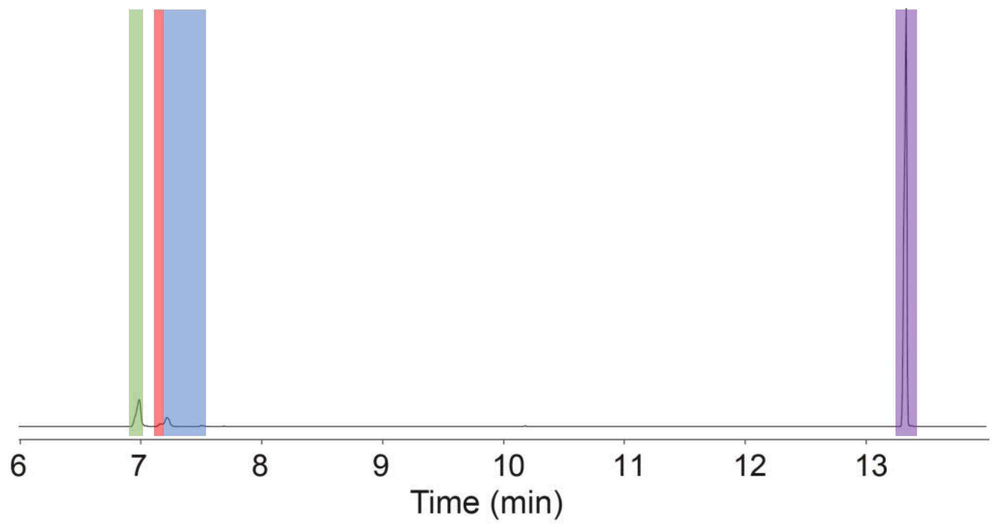

Analyte	Retention Time (min)	Integration (a.u)	Response Factor	Yield (%)
Isopulegol	6.987	816483	1.98	69.3
Citronellal	7.182	49783	1.98	4.3
Diastereomers	7.233-7.720	315448	1.98	26.4
Hexamethylbenzene	13.322	6401646	1.00	—

Figure S33. GC-FID trace of the carbonyl-ene cyclization of citronellal with Ph_4-P^NN^NP-$PdBF_4$ (0.5 mol % Pd) (0.2 mmol hexamethylbenzene internal standard)

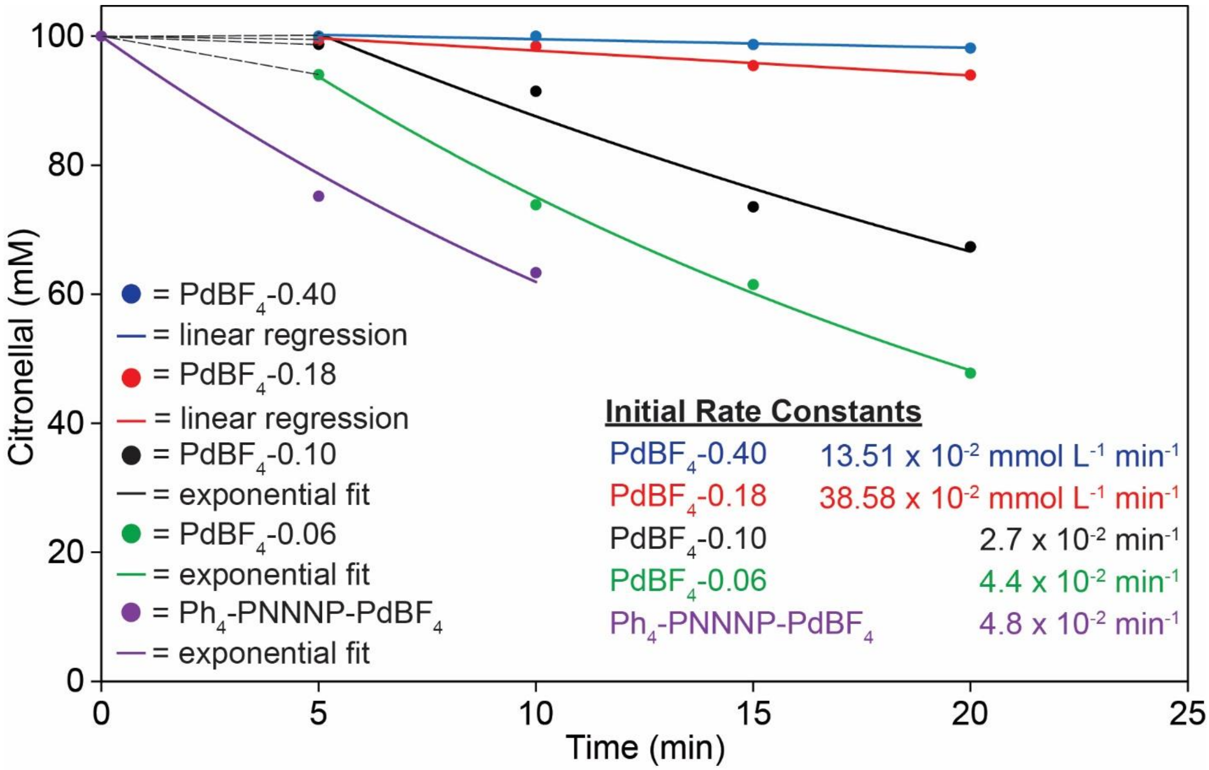

Figure S34. Initial rate constants calculated from the experimental data collected during the first time points for the cyclization of citronellal (100 mM) with the **$PdBF_4$-x** series and the homogenous catalyst Ph_4-P^NN^NP-$PdBF_4$ (0.5 mol % Pd)

Overview and Preparation of Homogenous Analogue Ph_4-PNNNP-$PdBF_4$

Ph_4-P^NN^NP-$PdBF_4$ was synthesized from Ph_4-P^NN^NP-PdI according to the method reported previously for tBu_4-P^NN^NP-$PdBF_4$.[12] Oxidative ligand exchange of I^- for BF_4^- was carried out using 5 equivalents of $NOBF_4$ in a DCM:MeCN (v/v 1:1) solvent mixture. The reaction was monitored by $^{31}P\{^1H\}$ NMR spectroscopy which showed the disappearance of the associated $[P^NN^NP\text{-PdI}]^+$ resonance at 73 ppm and appearance of a new resonance associated with $[P^NN^NP\text{-Pd-MeCN}]^+$ at 77 ppm. Minor resonances were observed at 75 ppm and 74 ppm consistent with partial iodination of the pyridyl backbone. Additionally, a minor resonance at 73 ppm consistent with $[P^NN^NP\text{-Pd-OH}]^+$ is observed owing to the presence of adventitious water.

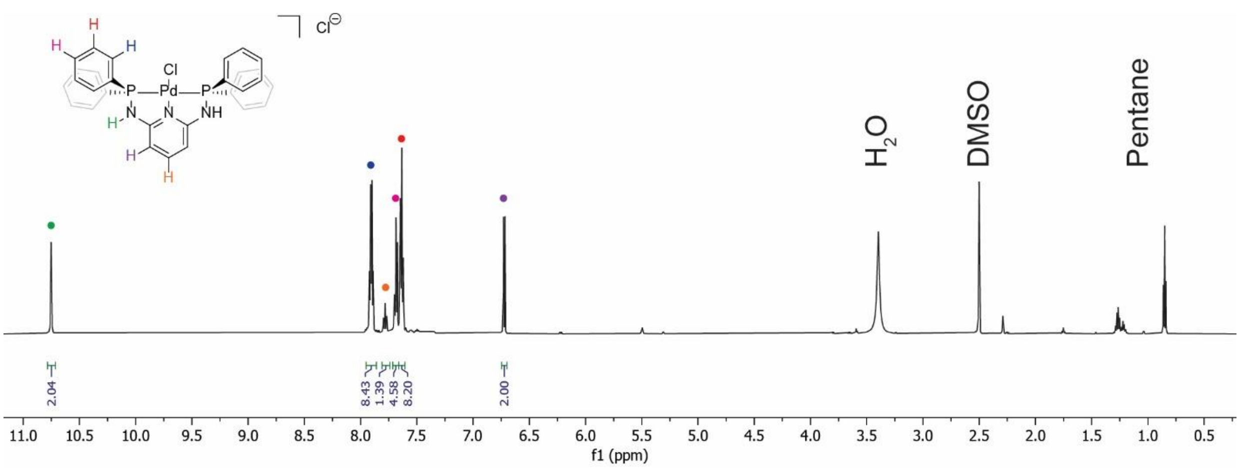

Figure S35. ^1H NMR spectrum (DMSO-d_6) of $[Ph_4\text{-}P^NN^NP\text{-PdCl}]Cl$

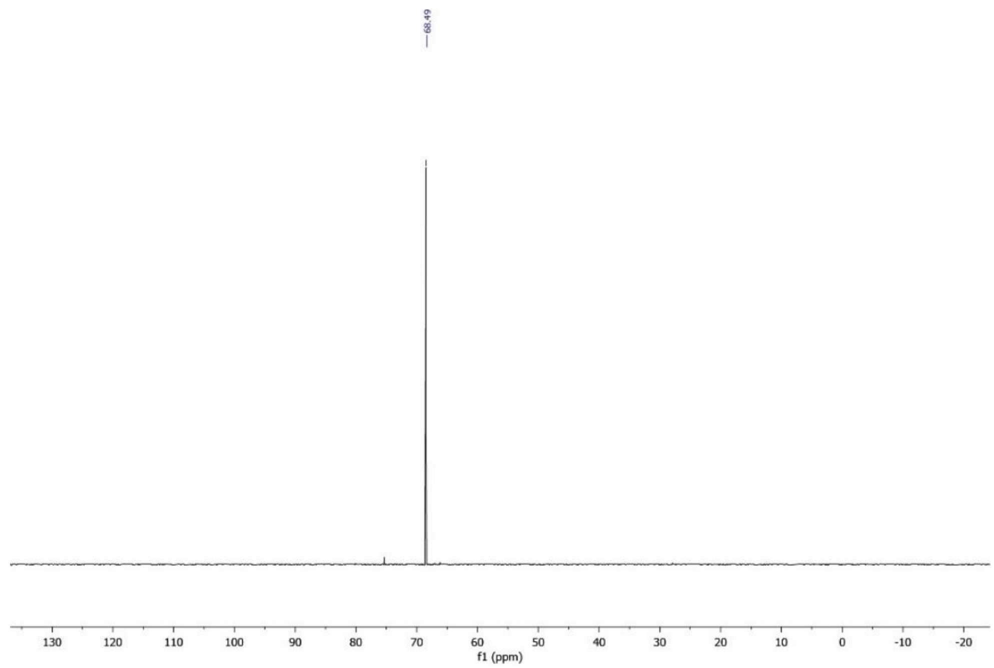

Figure S36. $^{31}P\{^1H\}$ NMR spectrum (DMSO-d_6) of [Ph$_4$-P^{N}N^{N}P-PdCl]Cl

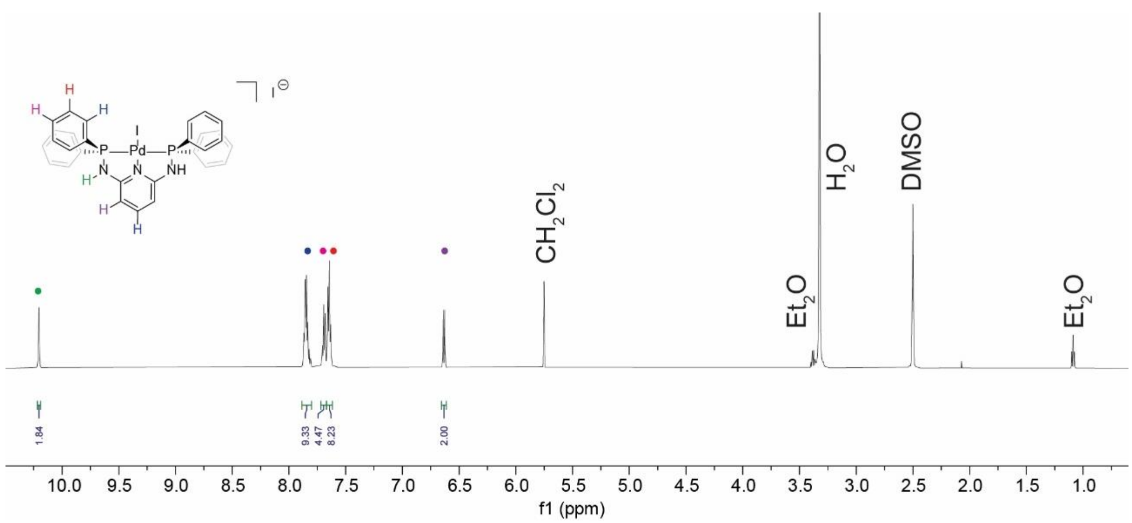

Figure S37. ^1H NMR spectrum (DMSO-d_6) of [Ph$_4$-P^{N}N^{N}P-PdI]I

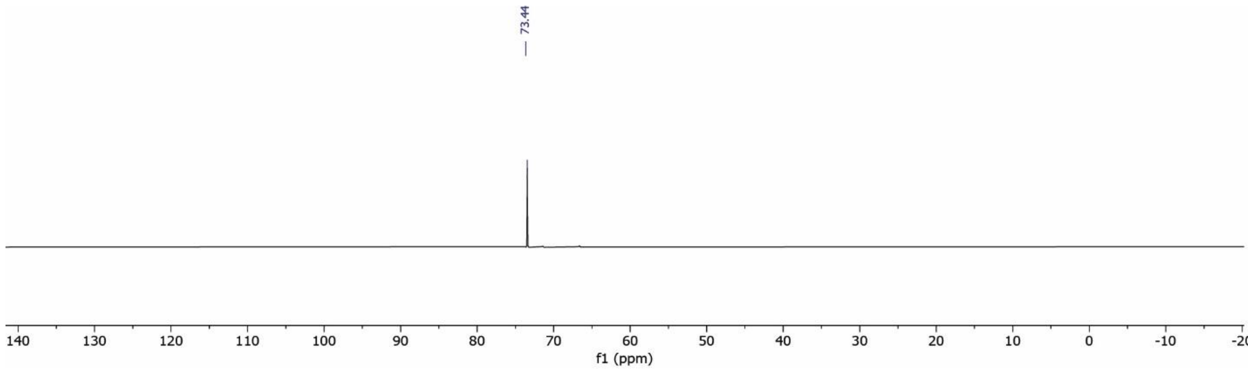

Figure S38. $^{31}P\{^1H\}$ NMR spectrum (DMSO-d$_6$) of [Ph$_4$-P^{N}N^{N}P-PdI]I

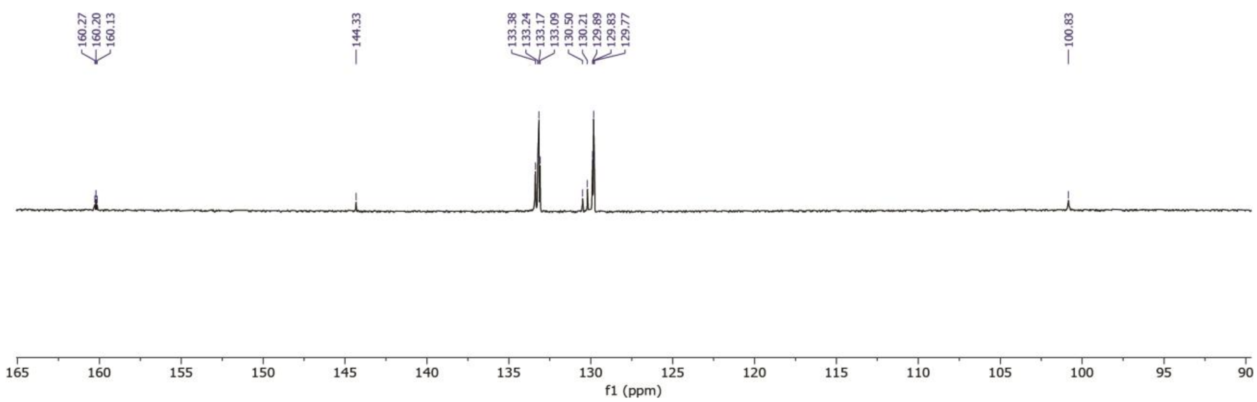

Figure S39. $^{13}C\{^1H\}$ NMR spectrum (DMSO-d$_6$) of [Ph$_4$-P^{N}N^{N}P-PdI]I

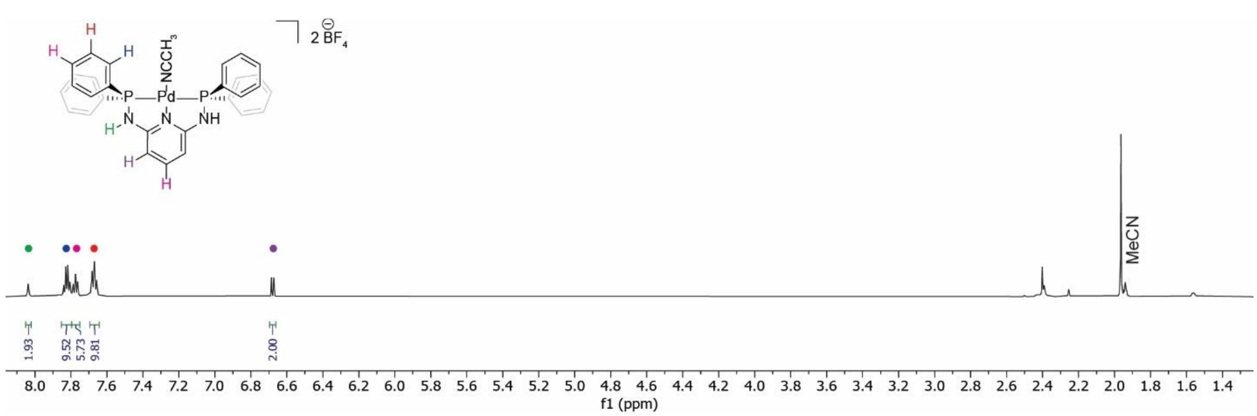

Figure S40. ^1H NMR spectrum (CD$_3$CN) of [Ph$_4$-P^{N}N^{N}P-Pd-MeCN][BF$_4$]$_2$

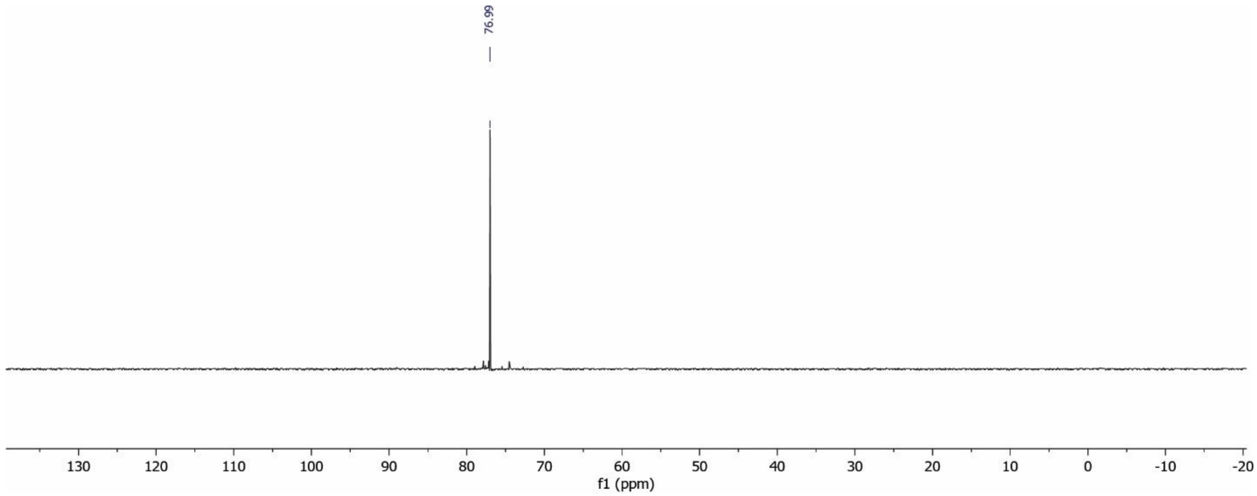

Figure S41. $^{31}P\{^{1}H\}$ NMR spectrum (CD_3CN) of $[Ph_4\text{-}P^NN^NP\text{-}Pd\text{-}MeCN][BF_4]_2$

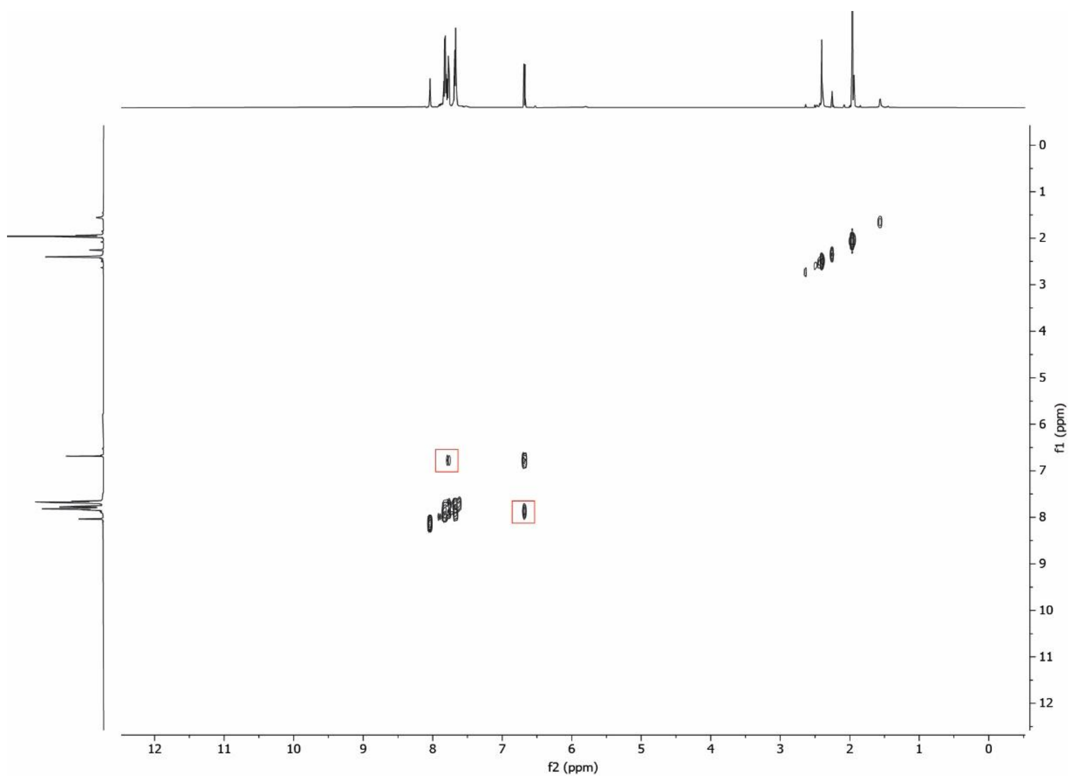

Figure S42. ^{1}H – ^{1}H COSY spectrum (CD_3CN) of $[Ph_4\text{-}P^NN^NP\text{-}Pd\text{-}MeCN][BF_4]_2$ with red boxes to indicate pyridine backbone cross peaks

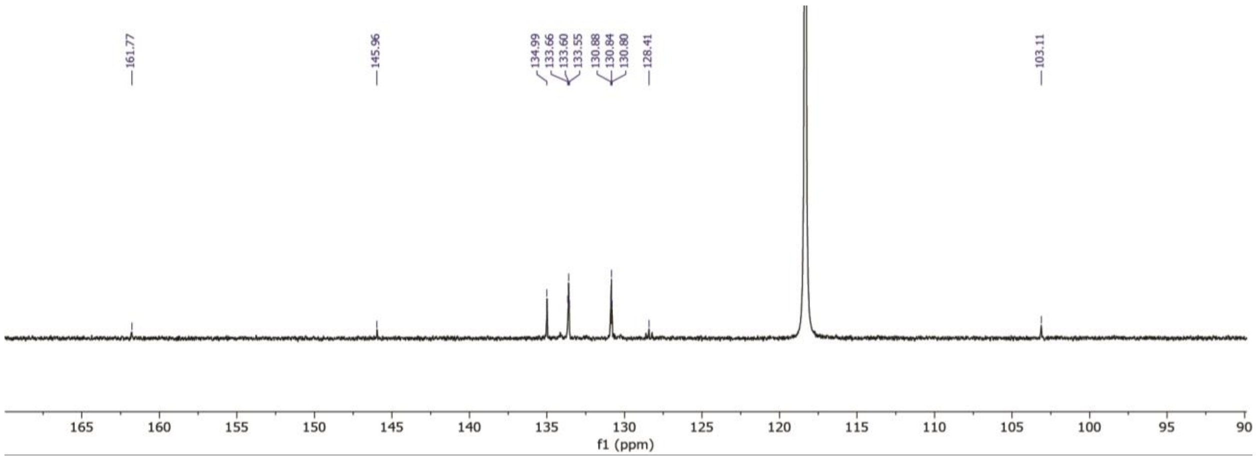

Figure S43. $^{13}C\{^1H\}$ NMR spectrum (CD_3CN) of $[Ph_4\text{-}P^NN^NP\text{-}Pd\text{-}MeCN][BF_4]_2$

References

1 A. Corma and M. Renz, *Chem. Commun.*, 2004, **4**, 550–551.

2 J. Jiang, F. Gándara, Y. B. Zhang, K. Na, O. M. Yaghi and W. G. Klemperer, *J. Am. Chem. Soc.*, 2014, **136**, 12844–12847.

3 M. Ermer, J. Mehler, B. Rosenberger, M. Fischer, P. S. Schulz and M. Hartmann, *ChemistryOpen*, 2021, **10**, 233–242.

4 F. Vermoortele, M. Vandichel, B. Van De Voorde, R. Ameloot, M. Waroquier, V. Van Speybroeck and D. E. De Vos, *Angew. Chem.Int. Ed.*, 2012, **51**, 4887–4890.

5 F. Vermoortele, B. Bueken, G. Le Bars, B. Van De Voorde, M. Vandichel, K. Houthoofd, A. Vimont, M. Daturi, M. Waroquier, V. Van Speybroeck, C. Kirschhock and D. E. De Vos, *J. Am. Chem. Soc.*, 2013, **135**, 11465–11468.

6 F. G. Cirujano and F. X. Llabrés I Xamena, *J. Phys. Chem. Lett.*, 2020, **11**, 4879–4890.

7 W.-L. Peng, F. Liu, X. Yi, S. Sun, H. Shi, Y. Hui, W. Chen, X. Yu, Z. Liu, Y. Qin, L. Song and A. Zheng, *J. Phys. Chem. Lett.*, 2022, **2**, 9295–9302.

8 F. G. Cirujano, F. X. Llabrés I Xamena and A. Corma, *Dalton Trans.*, 2012, **41**, 4249–4254.

9 A. M. Rasero-Almansa, M. Iglesias and F. Sánchez, *RSC Adv.*, 2016, **6**, 106790–106797.

10 L. Alaerts, E. Séguin, H. Poelman, F. Thibault-Starzyk, P. A. Jacobs and D. E. De Vos, *Chem. Eur. J.*, 2006, **12**, 7353–7363.

11 F. Vermoortele, R. Ameloot, L. Alaerts, R. Matthessen, B. Carlier, E. V. R. Fernandez, J. Gascon, F. Kapteijn and D. E. De Vos, *J. Mater. Chem.*, 2012, **22**, 10313–10321.

12 B. R. Reiner, A. A. Kassie and C. R. Wade, *Dalton Trans.*, 2019, **48**, 9588–9595.